Journal of Pharmacological Sciences 131 (2016) 172–183

Contents lists available at ScienceDirect

Journal of Pharmacological Sciences

journal homepage: www.elsevier.com/locate/jphs

Full paper

Haloperidol aggravates transverse aortic constriction-induced heart failure via mitochondrial dysfunction

Yasuharu Shinoda [a, 1], Hideaki Tagashira [a, 1], Md. Shenuarin Bhuiyan [b], Hideyuki Hasegawa [c, d], Hiroshi Kanai [c, d], Kohji Fukunaga [a, *]

[a] Department of Pharmacology, Graduate School of Pharmaceutical Sciences, Tohoku University, 6-3 Aramaki-Aoba, Aoba-ku, Sendai, Japan
[b] Department of Pathology and Translational Pathology, Louisiana State University Health Sciences Center, 1501 Kings Highway, Shreveport, LA 71103, USA
[c] Department of Electrical Engineering, Graduate School of Biomedical Engineering, Tohoku University, 6-6 Aramaki-Aoba, Aoba-ku, Sendai, Japan
[d] Department of Electrical Engineering, Graduate School of Engineering, Tohoku University, 6-6 Aramaki-Aoba, Aoba-ku, Sendai, Japan

ARTICLE INFO

Article history:
Received 19 April 2016
Received in revised form
25 May 2016
Accepted 27 May 2016
Available online 4 June 2016

Keywords:
Sigma-1 receptor (σ_1R)
Haloperidol
Angiotensin II (Ang II)
Myocardial hypertrophy
ATP

ABSTRACT

Haloperidol is an antipsychotic drug that inhibits the dopamine D2 receptor among others. Haloperidol also binds the sigma-1 receptor (σ_1R) and inhibits it irreversibly. A serious outcome of haloperidol treatment of schizophrenia patients is death due to sudden cardiac failure. Although the cause remains unclear, we hypothesized that these effects were mediated by chronic haloperidol inhibition of cardiac σ_1R. To test this, we treated neonatal rat cardiomyocytes with haloperidol, exposed them to angiotensin II and assessed hypertrophy, σ_1R expression, mitochondrial Ca^{2+} transport and ATP levels. In this context, haloperidol treatment altered mitochondrial Ca^{2+} transport resulting in decreased ATP content by inactivating cardiac σ_1R and/or reducing its expression. We also performed transverse aortic constriction (TAC) and then treated mice with haloperidol. After two weeks, haloperidol-treated mice showed enhanced heart failure marked by deteriorated cardiac function, reduced ATP production and increasing mortality relative to TAC only mice. ATP supplementation via sodium pyruvate rescued phenotypes seen in haloperidol-treated TAC mice. We conclude that σ_1R inactivation or downregulation in response to haloperidol treatment impairs mitochondrial Ca^{2+} mobilization, depleting ATP depletion from cardiomyocytes. These findings suggest a novel approach to mitigate haloperidol-related adverse effects in schizophrenia patients by ATP supplementation.

1. Introduction

Haloperidol was introduced as a therapeutic over 40 years ago and remains widely used clinically to treat acute and chronic psychosis, schizophrenia, and delirium. Antipsychotic activity of haloperidol is thought to be mediated, at least in part, by its antagonism (Ki = 2.8 nM) of the dopamine D2 receptor (8,30,52,56). In addition, haloperidol has comparable affinity for the sigma-1 receptor (σ_1R) and is known to act as a σ_1R inhibitor (Ki = 3.0 nM) (8,32); however, the consequences of haloperidol binding to σ_1Rs are less well known. Studies show that haloperidol administered at therapeutic doses (≥0.003 mg/kg), as is used in humans, can inhibit σ_1 receptors *in vivo* (38) and that treatment reportedly decreases the density of brain σ_1R in patients (38). Moreover, several studies show that haloperidol is metabolized *in vivo* to a reduced form with higher affinity (in the nanomolar range) for σ_1Rs (17,32,52); conversely, reduced haloperidol binds dopamine receptors with 85-fold lower affinity than haloperidol (Ki = 239 nM) (8). Acting as an antagonist, the reduced form can irreversibly inactivate σ_1Rs in guinea pig brain homogenates and in SH-SY5Y human neuroblastoma cells (10).

Although haloperidol is generally considered safe, a serious adverse effect of its use in schizophrenia patients is an abnormal heart rhythm called torsades de pointes (TdP) and QT prolongation (QTP), which can lead to sudden death from heart failure (14,24,42). These outcomes have been reported following either oral (18,29) or

* Corresponding author. 6-3 Aramaki-Aoba, Aoba, Sendai 980-8578, Japan. Tel.: +81 22 795 6837; fax: +81 22 795 6835.
E-mail address: kfukunaga@m.tohoku.ac.jp (K. Fukunaga).
Peer review under responsibility of Japanese Pharmacological Society.
[1] These authors contributed equally to this work.

http://dx.doi.org/10.1016/j.jphs.2016.05.012

intravenous (26) normal therapeutic doses of haloperidol or as a result of overdose (23). The Food and Drug Administration (FDA) reported a total of 70 cases of intravenous haloperidol administration-associated fatal events (like QTP and/or TdP) and has warned patients about these potential outcomes (34). Molecular mechanisms underlying cardiotoxic effects remain unclear. We proposed that adverse cardiac effects of haloperidol are mediated by inhibition of cardiac σ_1Rs, which we confirmed to be abundantly expressed in mouse heart (7,16). We also reported that σ_1R activity is potentially cardioprotective and have shown a direct relationship between reduced σ_1R expression and impaired heart function in a transverse aortic constriction (TAC) mouse model of left ventricular hypertrophy (47). Our work has confirmed that σ_1R stimulation with selective agonists like fluvoxamine or SA4503 in TAC mice improved cardiac function and reduced cardiac hypertrophy (50). We also showed that in rat heart, targeting σ_1R with neurosteroid dehydroepiandrosterone (DHEA) or pentazocine can promote cardioprotection in the context of pressure overload (PO)-induced cardiac dysfunction (44,46).

σ_1R is localized in the mitochondria-associated endoplasmic reticulum (ER) membrane (MAM) where it interacts with the inositol 1,4,5-trisphosphate receptor (IP_3R) to regulate Ca^{2+} transport from the ER lumen into mitochondria (22). Cardiomyocytes express all the three types of IP_3Rs (approximate relative abundance: IP_3R1, 25%; IP_3R2, 48%; and IP_3R3, 27%), and the three subtypes differ in function, expression pattern and subcellular localization in different cell types (1,53,55). We previously reported that perturbation of IP_3R-mediated Ca^{2+} release plays an important role in development of cardiac hypertrophy, and that σ_1R agonists modulate IP_3R-mediated Ca^{2+} release in cardiomyocytes (44,45). However, it is not known whether haloperidol-induced inactivation and/or reduction in expression of cardiac σ_1R would alter mitochondrial Ca^{2+} mobilization through IP_3R expressed in cardiomyocytes and thereby promote adverse cardiac effects.

In this study, we asked whether haloperidol treatment induced cardiotoxicity mediated by σ_1R inactivation. We discovered that haloperidol-induced σ_1R inactivation exacerbates Ang II-induced impairment of sarcoplasmic reticulum (SR)-mitochondrial Ca^{2+} transport, leading to decreases in mitochondrial ATP production, which in turn aggravated cardiac contractile dysfunction in TAC mice. Interestingly, co-administration of an ATP supplement such as sodium pyruvate restored cardiac ATP levels and ameliorated haloperidol-induced cardiac contractile dysfunction in TAC mice. This study suggests that co-administration of an ATP supplement with therapeutic doses of haloperidol could be beneficial in preventing adverse effects of haloperidol in schizophrenic patients.

2. Materials and methods

2.1. Materials

Reagents and antibodies were obtained from the following sources: anti-σ_1R antibody (Abcam, Cambridge, UK); anti-voltage-dependent anion channel (VDAC) antibody (Cell Signaling Technology, Beverly, MA); anti-p62 antibody (MBL, Nagoya, Japan); anti-LC3 antibody (MBL); anti-cytochrome c antibody (BD Biosciences, San Diego, CA); anti-β-tubulin antibody (Sigma, St. Louis, MO). Haloperidol was purchased from Dainippon Sumitomo Pharma Co. Ltd. (Osaka, Japan). Other reagents were of the highest quality available (Wako Pure Chemicals, Osaka, Japan). The σ_1R agonist SA4503 was synthesized in the Laboratory of Medicinal Chemistry, Zhejiang University (Hangzhou, China).

2.2. Animals and operations

All procedures for handling animals complied with the *Guide for Care and Use of Laboratory Animals* and were approved by the Animal Experimentation Committee of Tohoku University Graduate School of Pharmaceutical Sciences. Adult male ICR mice weighing 35–40 g were obtained from Nippon SLC (Hamamatsu, Japan). Ten-week-old males were acclimated to the local environment for 1 week, which included housing in polypropylene cages at 23 ± 1 °C in a humidity-controlled environment maintained on a 12-h light/dark schedule (lights on 8:00 AM–8:00 PM). Mice were provided food and water ad libitum. Transverse aortic constriction (TAC) was performed as described (44,50) on male ICR mice under anesthesia using a mixture of ketamine (100 mg/kg, i.p.) (Daiichi Sankyo Pharmaceutical Co. Ltd, Tokyo, Japan) and xylazine (5 mg/kg, i.p.) (Sigma). Adequate depth of anesthesia was confirmed by a negative toe-pinch reflex. If anesthesia was not sufficient, then a top-up dose of 20% of the initial dose was given.

2.3. Experimental design

ICR mice were randomly separated into seven experimental groups: 1) Sham (n = 5), 2) Sham plus sodium pyruvate (Pyr) treatment (1.0 mg/kg, p.o.) (n = 4), 3) Sham plus haloperidol (Halo) treatment (0.1 mg/kg, p.o.) (n = 6), 4) TAC plus vehicle treatment (n = 9), 5) TAC plus sodium pyruvate treatment (n = 5), 6) TAC plus haloperidol treatment (n = 10), and 7) TAC plus haloperidol plus sodium pyruvate treatment (n = 11). Vehicle, sodium pyruvate and haloperidol were administered orally for 2 or 4 weeks (once daily) using a metal gastric zonde for mice in a volume of 1 ml/100 g of mouse body weight, starting from the onset of aortic banding.

2.4. Echocardiography and measurement of cardiac hypertrophy

Noninvasive echocardiographic measurements were performed as described (47,50). Briefly, noninvasive echocardiographic measurements were performed in mice anesthetized with a mixture of ketamine (100 mg/kg, i.p.) and xylazine (5 mg/kg, i.p.) using ultrasonic diagnostic equipment (SSD-6500; Hitachi-Aloka, Tokyo, Japan) equipped with a 10-MHz linear array transducer (UST-5545; Hitachi-Aloka). The heart was imaged in the two-dimensional parasternal short-axis view, and an M-mode echocardiogram of the mid-ventricle was recorded at the level of the papillary muscles. Diastolic and systolic LV wall thickness, LV end-diastolic diameter (LVEDD), LV end-systolic diameter (LVESD) and ejection fraction (EF) were measured. All measurements were done from leading edge to leading edge according to the American Society of Echocardiography guidelines. The percentage of LV fraction shortening (FS) was calculated as ([LVEDD − LVESD]/LVEDD) × 100. Following sacrifice by cervical spine fracture dislocation, the thoracic cavity of mice was opened, and hearts were immediately harvested and weighed.

2.5. Cultured cardiomyocytes

Neonatal rat ventricular cardiomyocytes (NRVMs) were isolated from hearts of 1 to 3-day-old Wistar rat pups that had been sacrificed by decapitation, and cardiomyocytes were cultured as described (47,50). In the experiments that followed, cells were stimulated with Ang II (100 nM), haloperidol (10 nM) or SA4503 (1 μM) for 1 or 48 h.

2.6. Morphological analysis, immunocytochemistry of cultured cardiomyocytes and histological analysis of cardiac tissues

Morphological analysis was performed as described (44). The surface area of control cells was defined as 100% and then compared with that of treated cells. For mitochondrial staining, cells were stained for 20 min with 0.02 μM Mito Tracker Red CMXRos (Molecular Probes, Eugene, OR) before fixation (12). After permeabilization with 0.1% Triton X-100 in PBS, fixed cells were incubated with 1% bovine serum albumin (BSA) (Sigma) in PBS for 30 min. For immunocytochemistry, cells were incubated 24 h at 4 °C with anti-LC3 antibody (1:500), anti-p62 antibody (1:500) or anti-cytochrome c antibody (1:500) in PBS containing 1% BSA. After washing, cells were incubated 24 h with Alexa 488-conjugated anti-rabbit IgG and Alexa 488-conjugated phalloidin and/or Alexa 594-conjugated anti-mouse IgG (Invitrogen, Carlsbad, CA) in PBS containing 1% BSA. For nuclear staining, sections were incubated with 4′,6-diamidino-2-phenylindole dihydrochloride (DAPI) (Sigma; 1 μg/mL PBS). Immunofluorescent images were analyzed using a confocal laser scanning microscope (LSM700; Zeiss, Thornwood, NY). Quantitative analyses of cell size, fluorescence intensity of Mito Tracker and LC3 granules were undertaken using ImageJ software. Specifically, after image capture, lines surrounding each cell were drawn and signal intensity inside those lines was determined using ImageJ software.

Histological analysis was performed as described (44). Briefly, fixed and dehydrated murine heart was embedded in O.C.T. compound (Sakura Finetek, Torrance, CA) and sliced. For Masson's trichrome staining, 20-μm slice tissues were stained using a Trichrome Stain (Masson) Kit (Sigma) according to manufacturer's protocol.

2.7. Western blot analysis and measurement of ATP content

Dissected LV tissue samples were rapidly frozen in liquid nitrogen and stored at −80 °C before analysis (47). In the case of cardiomyocytes, cells were washed with PBS at 4 °C and stored at −80 °C until immunoblotting was performed as described (46,50). For assays, each frozen sample was homogenized as described (44,49). ATP measurement was performed using an ATP assay kit (Toyo Ink, Tokyo, Japan), according to the manufacturer's protocol (50). Briefly, frozen samples were homogenized in homogenate buffer (0.25M sucrose, 10 mM HEPES-NaOH: pH 7.4), and lysates were cleared by centrifugation at 1000 g for 10 min at 4 °C. The supernatant was collected, and supernatant proteins were solubilized in extraction buffer. After 30 min, luciferin buffer was added to each sample and oxyluciferin was detected using a luminometer (Gene Light 55, Microtec, Funabashi, Japan).

2.8. Real-time PCR

Total RNA from LV tissues was isolated using TRI Reagent (Sigma). Briefly, LV tissues were homogenized in TRI Reagent and passed through 23-gauge needle ten times on ice. Chloroform was added to homogenates, and the mixture was kept on ice for 15 min and then centrifuged at 15,000 rpm for 5 min at 4 °C. The top layer of supernatant was collected and combined with one volume of isopropanol and then centrifuged at 15,000 rpm for 20 min at 4 °C. Resulting RNA pellets were washed with 75% ethanol and suspended in sterile water containing 0.1% diethyl pyrocarbonate (Sigma) to block RNA degradation. cDNAs were synthesized by reverse transcription as described (40). Real-time PCR was performed with iQ CYBR Green Supermix (Bio-Rad Laboratories, Redmond, WA) following the manufacturer's protocol. The primers were: mouse forward Anp, 5′- GTCCAACACAGATCTGATGG -3′; reverse Anp, 5′- GATTTGGCTGTTATCTTCGG -3′; mouse Gapdh forward, 5′- TGTGTCCGTCGTGGATCTGA -3′; and reverse Gapdh, 5′- CACCACCTTCTTGATGTCATCATAC -3′.

2.9. Measurement of intracellular Ca^{2+} levels

NRVMs were cultured on 0.01% poly-L-lysine (Sigma)-coated glass-bottom dishes and maintained in growth medium. After stimulation with 100 nM Ang II for either 48 or 72 h, myocytes were loaded with the Ca^{2+}-sensitive dye Fura-2 acetoxymethyl ester (2.5 μM; Sigma) for 30 min before measuring Ca^{2+} levels in a chamber on an inverted microscope stage. Cells were perfused with normal Tyrode solution containing 150 mM NaCl, 4 mM KCl, 1 mM $MgCl_2$, 2 mM $CaCl_2$, 5.6 mM glucose, and 5 mM HEPES at 37 °C. When Ca^{2+} fluorescence levels reached a steady state, 10 μM phenylephrine (PE) or 10 μM ATP was applied for 10 s through a small perfusion pipe. The amplitude of the PE- or ATP-induced Ca^{2+} transient was used as an index of IP_3R-mediated Ca^{2+} release. Changes in PE- or ATP-induced Ca^{2+} release from the SR were determined using the ratio of fluorescence emission at 530 nm in response to excitation at 340 nm and to that at 380 nm.

2.10. Measurement of mitochondrial Ca^{2+} levels

NRVMs were cultured on 0.01% poly-L-lysine (Sigma)-coated glass-bottom dishes and maintained in growth medium. Transfections were performed with ratiometric-pericam targeted to the mitochondrial matrix (ratiometric-pericam-mt/pcDNA3), which was a kind gift of Dr. Atsushi Miyawaki of the RIKEN Brain Science Institute (Wako, Japan) (35,40,50). Briefly, 1 μg/μL ratiometric-pericam-mt/pcDNA3 in 1 μL was added to 199 μL opti-MEM (Invitrogen), and 1 μl Lipofectamine 2000 (Invitrogen) was added to 9 μL opti-MEM. Both solutions were incubated separately at room temperature for 5 min and then mixed and incubated at room temperature for 15–20 min. Cells were incubated with 800 μL of opti-MEM to which 200 μL of the ratiometric-pericam-mt/pcDNA3 solution had been added. Cells were then incubated at 37 °C in a 5% CO_2 atmosphere for 4 h to initiate transfection. Then, 500 μl DMEM supplemented with 5% FBS was added to each well to maintain cell viability. After 24 h, 100 nM Ang II was added. After stimulation for 48 h, cells were perfused with normal Tyrode solution at 37 °C. When Ca^{2+} fluorescence levels reached a steady state, 10 μM PE or 10 μM ATP was applied for 10 s through a small perfusion pipe. Dual-excitation imaging with ratiometric-pericam-mt required two filters (EX:482/35, DM:506, EM:536/40 and EX:414/46, DM:510, EM:527/20). Changes in PE- or ATP-induced Ca^{2+} transport from the SR to mitochondria were determined using the Metafluor Imaging system (Molecular Devices, Sunnyvale, CA).

2.11. TUNEL staining

Double-staining for TUNEL to detect apoptotic cell nuclei and propidium iodide to detect myocardial cell nuclei was described previously (40). TUNEL staining was performed using an in situ apoptosis detection kit (Takara Bio Inc., Shiga, Japan), according to the manufacturer's protocol. Cardiomyocytes from at least four randomly selected slides per block were evaluated immunohistochemically to determine the number and percentage of cells exhibiting staining indicative of apoptosis. The index of apoptosis (number of apoptotic myocytes/the total number of myocytes counted × 100%) was determined.

2.12. Statistical analysis

Values are represented as means ± standard error of the mean (S.E.M.). Comparison between two experimental groups was made

using the unpaired Student's *t* test to evaluate effects of SA4503 on cardiomyocyte size. In other experiments, differences were evaluated using analysis of variance (ANOVA) followed by multiple comparisons using Dunnett's test, except for NRVM morphological measurement. Results related to NRVM area were evaluated by Scheffe's test to test the effect of SA4503. Survival probability was calculated by Kaplan–Meier analysis, and statistical significance was analyzed by Log-rank test. $P < 0.05$ was considered statistically significant. F and P values are reported in corresponding figure legends.

3. Results

3.1. Haloperidol treatment of cultured cardiomyocytes enhances Ang II-induced hypertrophy and mitochondrial dysfunction

We previously reported that σ_1R is abundantly expressed in rodent cardiomyocytes and showed that σ_1R activation with a variety of agonists was cardioprotective *in vitro* and *in vivo* (2–4,44–47,50). Thus, we reasoned that haloperidol, acting as an irreversible σ_1R antagonist, could aggravate Ang II-induced hypertrophy via σ_1R inactivation (10) and/or by reducing σ_1R expression in cardiomyocytes (38). To assess this possibility, we first observed the size of NRVMs exposed to Ang II (100 nM) for 48 h with or without haloperidol treatment. Treatment with Ang II only significantly increased cell size relative to that of untreated controls ($P < 0.05$ vs. control) (Fig. 1A and B). Haloperidol treatment (10 nM) significantly enhanced Ang II-induced cell enlargement ($P < 0.01$ vs. control; $P < 0.05$ vs. Ang II) (Fig. 1A and B). Haloperidol treatment alone also induced cardiomyocyte hypertrophy in mock-treated controls ($P < 0.05$ vs. control) (Fig. 1A and B). Interestingly, haloperidol treatment of Ang II-exposed cells for 48 h significantly reduced expression of σ_1R protein ($P < 0.05$ vs. control) (Fig. 1D), but treatment with either haloperidol or Ang II did not (Fig. 1D). To confirm that σ_1R activity was relevant to these effects, we employed the selective σ_1R agonist (SA4503) (33). SA4503 co-administration (1 μM) with haloperidol rescued haloperidol-induced cardiomyocyte hypertrophy ($P < 0.01$ vs. haloperidol

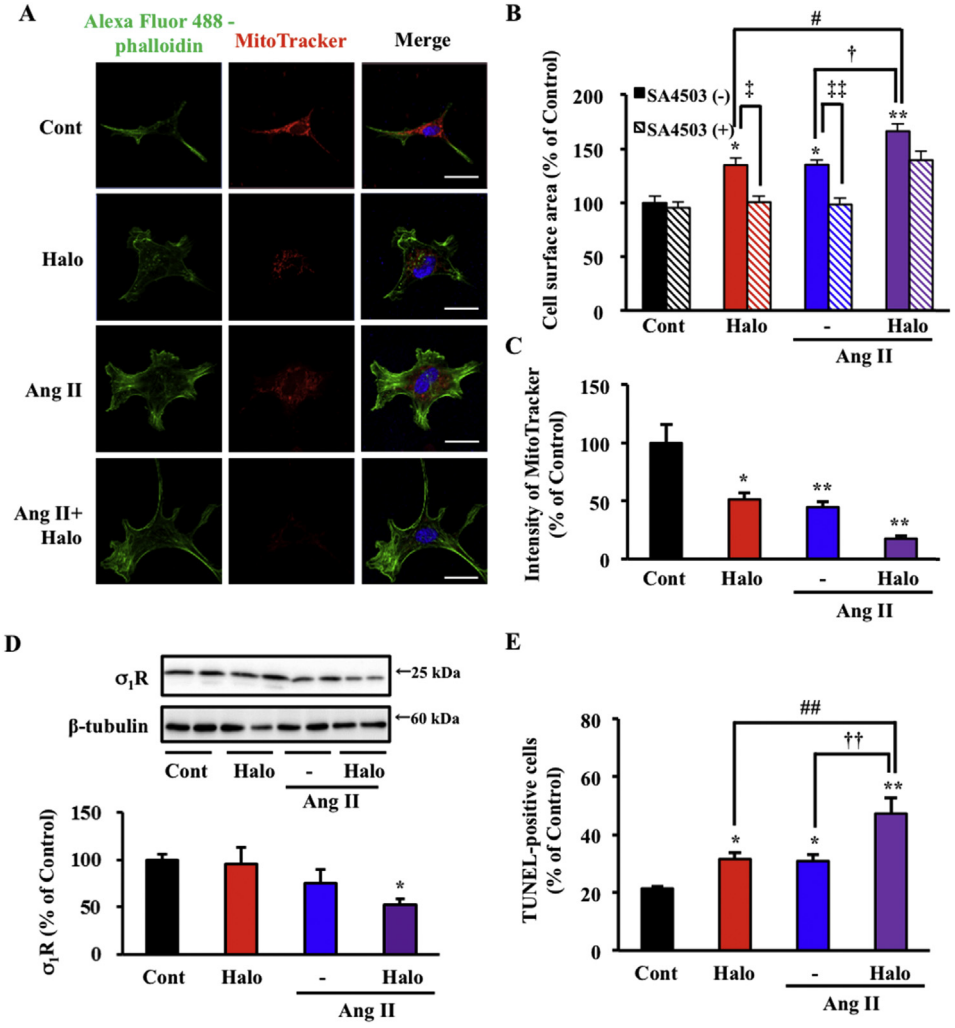

Fig. 1. Effects of haloperidol treatment on Ang II-induced hypertrophy and mitochondrial structure in cultured cardiomyocytes. A: Cells were stained with Alexa Fluor 488-phalloidin (green), Mito Tracker Red CMXRos (red) and DAPI (blue) and assessed by fluorescence microscopy. B: Cell size is expressed as a percentage of surface area relative to untreated control cells. Fifty cells were counted in each experiment. $F(7, 408) = 18.680$, $P < 0.01$. C: Mito Tracker Red CMXRos intensity is expressed as a percentage of surface area relative to untreated control cells. Six to nine randomly selected fields were counted in each experiment. $F(3, 26) = 10.430$, $P < 0.01$. D: Upper, Immunoblot of σ_1R protein in NRVMs treated 48 h with or without Ang II or haloperidol (Halo). β-tubulin staining serves as a loading control. Lower, Densitometry analysis of σ_1R immunoreactive bands. Groups consist of 4 samples. E: TUNEL-positive cells were counted in cultures treated 48 h with or without Ang II or Halo. Eighty cells from 10 randomly selected fields were counted in each experiment. $F(3, 19) = 3.086$, $P < 0.05$. Data are expressed as percentages of control values (mean ± S.E.M.).*, $P < 0.05$ and **, $P < 0.01$ vs. control cells; #, $P < 0.05$ and ##, $P < 0.01$ vs. Halo-treated cells; †, $P < 0.05$ and ††, $P < 0.01$ vs. Ang II-treated cells; ‡, $P < 0.05$ and ‡‡, $P < 0.01$ vs. SA4503 (−) control.

treatment) (Fig. 1B). Both SA4503 and haloperidol block [^{3}H](+)-pentazocine binding to σ_1R (32,33), suggesting they occupy the same binding site. Therefore, SA4503 treatment at a relatively high concentration (1 μM) was sufficient to inhibit haloperidol (10 nM) binding in σ_1R-induced function. These findings suggest that haloperidol directly acts on the cardiac σ_1R to enhance Ang II-induced cardiomyocyte enlargement.

We have also reported that treatment of cardiomyocytes with σ_1R agonists has antihypertrophic effects in part by preventing mitochondrial dysfunction (45,50). We extended that analysis to define effect of σ_1R signaling on mitochondrial membrane potential under stress conditions, as assessed by Mito Tracker Red CMXRos staining. Staining intensity of cells treated with Ang II or haloperidol significantly decreased compared to that of untreated control cells (44.8% and 51.4% of control, respectively) ($P < 0.05$ and 0.01 for haloperidol and Ang II, respectively) (Fig. 1A and C). Treatment with both haloperidol and Ang II significantly reduced mitochondrial membrane potential ($P < 0.01$ vs. control) (Fig. 1A and C). We also investigated a potential effect of haloperidol on Ang II-induced cardiomyocyte apoptosis in cultured cardiomyocytes. Ang II or

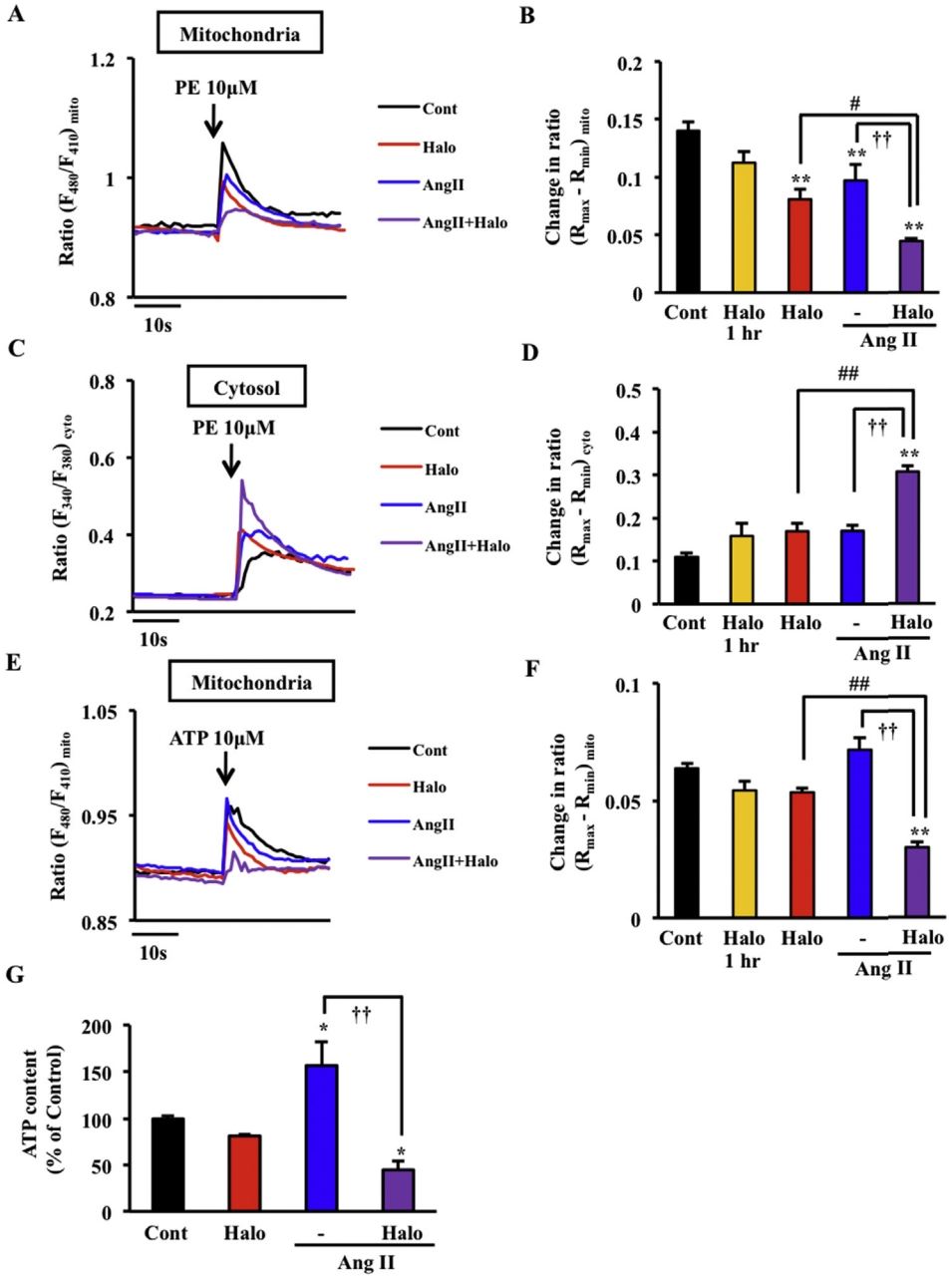

Fig. 2. Effects of haloperidol treatment on phenylephrine (PE) and ATP-induced Ca^{2+} influx into mitochondria and the cytosol and on ATP content. A: Time course of PE-induced Ca^{2+} influx into mitochondria treated 48 h with or without Ang II or Halo. B: Peak increases in $[Ca^{2+}]_{mito}$ induced by 10 μM PE. $F(4, 96) = 14.392$, $P < 0.01$. C: Time courses of PE-induced Ca^{2+} release into the cytosol in cells treated 48 h with or without Ang II or Halo. D: Peak increases in $[Ca^{2+}]_{cyto}$ induced by 10 μM PE. $F(4, 89) = 16.579$, $P < 0.01$. E: Time course of ATP-induced Ca^{2+} influx into mitochondria in cells treated 48 h with or without Ang II. F: Peak increases in $[Ca^{2+}]_{mito}$ induced by 10 μM ATP. Each group consists of >10 cells. $F(4, 101) = 20.761$, $P < 0.01$. G: Measurement of cellular ATP content with or without Ang II or Halo treatment. Groups consist of 3–4 samples. $F(3, 22) = 9.870$, $P < 0.01$. Data are expressed as percentages of control cell value (mean ± S.E.M.). *, $P < 0.05$ and **, $P < 0.01$ vs. control cells; #, $P < 0.05$ and ##, $P < 0.01$ vs. Halo-treated cells; ††, $P < 0.01$ vs. Ang II-treated cells.

haloperidol treatment for 48 h significantly increased cardiomyocyte apoptosis, as indicated by a relative increase in the number of TUNEL-positive cells ($P < 0.05$ vs. control for both treatments), while treatment with both significantly enhanced cardiomyocyte apoptosis ($P < 0.01$ vs. Ang II) (Fig. 1E).

3.2. Effect of haloperidol treatment on phenylephrine (PE)-induced Ca^{2+} mobilization and ATP content in NRVMs

We previously reported that σ_1R activation by agonists regulates IP_3R-mediated Ca^{2+} release in cardiomyocytes (45,50). Therefore, we examined the effects of haloperidol treatment on PE-induced IP_3R-mediated Ca^{2+} mobilization into mitochondria and cytosol in Ang II-treated cells. Treatment with haloperidol alone for 1 h slightly suppressed PE-induced mitochondrial Ca^{2+} transport relative to controls, an effect that was significant after 48 h of treatment ($P < 0.01$ for Halo) (Fig. 2A and B). Ang II treatment for 48 h severely impaired PE-induced mitochondrial Ca^{2+} transport compared to untreated control cells ($P < 0.01$ vs. control) (Fig. 2A and B). Treatment with haloperidol plus Ang II for 48 h significantly enhanced the Ang II response ($P < 0.01$ vs. Ang II) (Fig. 2A and B). We also examined the effects of haloperidol on PE-induced IP_3R-mediated Ca^{2+} release to the cytosol. Neither haloperidol nor Ang II treatment alone for 1 h or 48 h had a significant effect (Fig. 2C and D); however, combined administration of haloperidol plus Ang II for 48 h significantly increased PE-induced Ca^{2+} release to the cytosol ($P < 0.01$ vs. control and vs. Ang II) (Fig. 2C and D). We also examined the effects of haloperidol on IP_3R-mediated mitochondrial Ca^{2+} mobilization by supplementing Ang II-treated cells with ATP. Treatment with either haloperidol for 1 or 48 h or Ang II alone for 48 h had little effect on ATP-induced Ca^{2+} release to mitochondria (Fig. 2E and F). However, combining haloperidol with Ang II treatment for 48 h significantly impaired ATP-induced mitochondrial Ca^{2+} transport ($P < 0.01$ vs. Ang II) (Fig. 2E and F). These results suggest overall that haloperidol enhances Ang II-induced impairment of Ca^{2+} mobilization in both mitochondria and cytosol.

We next asked whether σ_1R inactivation by haloperidol impaired mitochondrial ATP production in NRVMs. Treatment with haloperidol alone slightly reduced ATP content relative to untreated control cells (Fig. 2G). Consistent with our previous study (45), Ang II exposure for 48 h increased ATP content ($P < 0.01$ vs. control) (Fig. 2G). Interestingly, treatment with haloperidol and Ang II treatment significantly decreased ATP content relative to Ang II treatment alone ($P < 0.01$ vs. Ang II) (Fig. 2G). In naive NRVMs, ATP-induced mitochondrial Ca^{2+} transport was significantly suppressed following acute haloperidol treatment for 1 h ($P < 0.05$ vs. control), while co-administration of haloperidol with the σ_1R agonist SA4503 eliminated this effect (Fig. 3A and B). By contrast, ATP-induced Ca^{2+} release to the cytosol was significantly potentiated by haloperidol treatment ($P < 0.01$ vs. control), which antagonized by SA4503 co-administration ($P < 0.01$ vs. Halo) (Fig. 3C and D). These observations suggest that σ_1R inactivation deregulates mitochondrial Ca^{2+} mobilization by decreasing ATP content, an outcome that may underlie haloperidol-induced cardiotoxicity.

3.3. Effects of haloperidol treatment on autophagy and mitochondrial integrity

Recent reports demonstrate that in cardiomyocytes, multiple forms of stress, including pressure overload, chronic ischemia, and ischemia-reperfusion, stimulate increased autophagy, a maladaptive response that contributes to heart failure (31,36,57). Given that Ang II and haloperidol co-administration alters mitochondrial Ca^{2+} transport and ATP production, we hypothesized that these effects

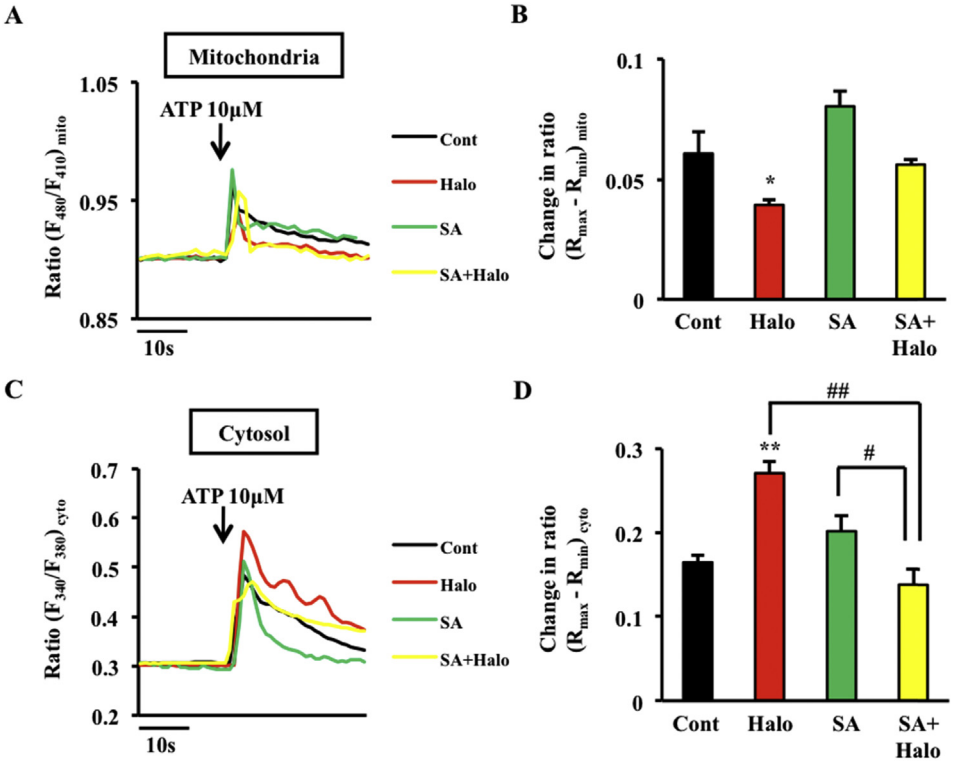

Fig. 3. Effects of acute haloperidol or SA4503 treatment on ATP-induced Ca^{2+} mobilization into mitochondria and the cytosol. A: Time course of ATP-induced Ca^{2+} influx into mitochondria in cardiomyocytes treated with or without Halo or SA4503 (SA) for 1 h. B: Peak increases in $[Ca^{2+}]_{mito}$ induced by 10 μM ATP. $F(3, 71) = 4.281$, $P < 0.01$. C: Time courses of ATP-induced Ca^{2+} release to the cytosol. D: Peak increases in $[Ca^{2+}]_{cyto}$ induced by 10 μM ATP. Groups consist of >10 cells. $F(3, 55) = 7.789$, $P < 0.01$. Data are expressed as percentages of control value (mean ± S.E.M.). *, $P < 0.05$ and **, $P < 0.01$ vs. control cells; #, $P < 0.05$ and ##, $P < 0.01$ vs. Halo-treated cells.

may be due to increased autophagic activity. We assessed this possibility by monitoring the autophagic marker LC3 in cardiomyocytes treated with or without Ang II and/or haloperidol. Ang II treatment alone for 48 h induced a significant increase in the intensity of punctate LC3-positive dots ($P < 0.01$ vs. control) (Fig. 4A and B). Moreover, treatment with both haloperidol and Ang II significantly enhanced induction of LC3-positive dots ($P < 0.05$ vs. Ang II) (Fig 4A and B), a finding consistent with earlier studies (57). Accordingly, we observed induction of expression of p62, a different marker of autophagy, in cardiomyocytes treated with Ang II, haloperidol or both (Fig. 4C). Treatment of cardiomyocytes with a combination of haloperidol and Ang II also elicited a fragmented staining pattern of the mitochondrial marker, cytochrome c, which preferentially distributes in tubular and branching pattern in untreated control cells (Fig. 4A). Fragmented cytochrome c staining partially co-localized with LC3 granules, suggesting that mitochondria are undergoing mitophagy. We next asked whether apparent mitochondrial degradation occurred in cardiomyocytes treated with or without Ang II and/or haloperidol. Combined treatment with both for 48 h significantly decreased expression of voltage-dependent anion channel (VDAC), a mitochondrial protein critical for Ca^{2+} transport with IP_3R ($P < 0.05$ vs. control and $P < 0.01$ vs. Ang II) (Fig. 4D and E). Taken together, our findings suggest that chronic haloperidol treatment has deleterious effects on mitochondrial integrity via induction of autophagy in cardiomyocytes.

3.4. Effects of haloperidol and sodium pyruvate administration on cardiac hypertrophy and dysfunction in TAC mice

To assess the effect of haloperidol *in vivo*, we treated both sham-operated and TAC mice with daily oral administration of haloperidol (0.1 mg/kg) beginning two days after surgery. Two weeks later, treatment groups were analyzed for myocardial hypertrophy based on assessment of heart weight-to-body weight (HW/BW) ratio, lung weight-to-body weight (LW/BW) and mRNA levels of atrial natriuretic peptide (ANP), a hypertrophy marker (Fig. 5A–C). TAC mice showed significantly increased HW/BW and ANP mRNA levels and moderately increased LW/BW compared to sham mice ($P < 0.01$ vs. sham-vehicle in HW/BW and ANP mRNA) (Fig. 5A–C). Furthermore, haloperidol treatment (0.1 mg/kg) of TAC mice significantly increased the LW/BW ratio ($P < 0.01$ vs. sham-vehicle for TAC-haloperidol), an effect not seen in vehicle-treated TAC controls (Fig. 5B). Given that haloperidol treatment perturbs mitochondrial ATP production, we supplemented TAC animals with sodium pyruvate (1.0 mg/kg) to determine whether the haloperidol effect was due to decreased mitochondrial function. Interestingly, treatment with both sodium pyruvate (1.0 mg/kg) and haloperidol prevented TAC and/or haloperidol-induced cardiac hypertrophy ($P < 0.01$ vs. TAC-haloperidol) (Fig. 5A–C).

To assess a potential effect of haloperidol treatment on cardiac remodeling, we measured cardiac fibrosis using Masson's trichrome staining. Interestingly, we observed adverse cardiac remodeling, as indicated by induction of interstitial fibrosis, following chronic oral administration of haloperidol to TAC mice, an affect blocked by co-administration of sodium pyruvate (Fig. 5D). We also assessed cardiac function by echocardiography after similar treatments (Fig. 5E). Control vehicle-treated TAC mice showed slightly decreased LC fractional shortening (FS) and ejection fraction (EF) at 2 weeks after surgery, consistent with our previous report (47). By contrast, TAC mice treated with haloperidol showed significant cardiac dysfunction, as indicated by decreased FS and EF, compared to vehicle-treated sham mice ($P < 0.01$ vs. sham-vehicle) (Fig. 5F and G). All groups showed comparable LVESD values [$F(6, 44) = 1.961$, $P = 0.0920$] (Fig. 5H), haloperidol treatment on TAC mice elicited only a slight increase in LVESD. These results suggest that haloperidol induces some indications of cardiac dysfunction in TAC mice, such as increased LW/BW ratio (Fig. 5B). Interestingly, co-administration of sodium pyruvate with haloperidol prevented haloperidol-induced deterioration of cardiac function and progression of heart failure ($P < 0.01$ vs. TAC-haloperidol in FS and EF; $P < 0.05$ vs. TAC-haloperidol in LVESD) (Fig. 5E–H). Taken together, we conclude that haloperidol-induced progression of heart failure is mediated by reduced ATP production *in vivo*.

3.5. Effects of haloperidol plus sodium pyruvate treatment on cardiac σ_1R expression, ATP content and TAC mouse survival

Earlier studies had reported that haloperidol treatment of human subjects was accompanied by a decrease in the density of σ_1R expression in brain (38). Therefore, we asked whether mice chronically treated with haloperidol would also exhibit similar changes in expression pattern in cardiac tissue. Interestingly, after 2 weeks of haloperidol administration, TAC mice showed significantly decreased cardiac σ_1R expression ($P < 0.01$ vs. sham-vehicle) (Fig. 6A and B), although untreated and haloperidol-treated sham mice showed comparable receptor expression (Fig. 6A and B). These data suggest that cardiac defects seen in TAC mice treated with haloperidol may be due to decreased σ_1R expression.

When we examined effects on ATP production we found that haloperidol treatment of TAC mice significantly decreased cardiac ATP levels relative to sham or TAC mice ($P < 0.01$ vs. TAC-vehicle) (Fig. 6C). Interestingly, treatment with sodium pyruvate plus haloperidol significantly and restored ATP content in heart ($P < 0.05$ vs. TAC-haloperidol) but did not rescue decreased σ_1R expression ($P < 0.05$ vs. sham-vehicle) (Fig. 6A–C). Furthermore, Kaplan–Meier survival analysis showed that chronic haloperidol treatment increased mortality of TAC mice, with a survival rate of 50% at 14 days and 33% at 28 days ($P < 0.05$ vs. TAC-vehicle) compared to 86% survival at 28 days seen in TAC only mice (Fig. 6D). Sham mice treated with haloperidol showed 100% survival. Co-administration of sodium pyruvate with haloperidol to TAC mice prevented haloperidol-induced progression of heart failure and significantly improved mortality ($P < 0.05$ vs. TAC-haloperidol). These correlative observations strongly suggest that deleterious cardiac effects seen following chronic haloperidol treatment of TAC mice are mediated by decreased σ_1R expression and/or inactivation, which in turn promote decreased mitochondrial ATP production.

4. Discussion

Recently, we have been exploring the potential beneficial effect of σ_1R agonists on the heart, effects which were heretofore underappreciated. Despite the numerous studies analyzing the effects of σ_1R ligands in heart tissues, we still do not fully understand how σ_1R function is perturbed in pathological states and whether σ_1R exists as active state or resting state without stimulation of σ_1R ligands. Here, to understand σ_1R function in heart, we investigated temporal changes in its expression levels in murine models of cardiac hypertrophy and heart failure. We have reported that along with progression of LV hypertrophy, σ_1R expression was significantly reduced in the heart and showed a significant positive linear correlation with heart function (6,47). Our previous studies clearly demonstrated that σ_1R activation by selective agonists is cardioprotective in rodent models of cardiac hypertrophy and heart failure (2–7,44–50) Here, we addressed the deleterious effects of chronic σ_1R inactivation and decreased expression in heart brought on by treatment with haloperidol in the progression of heart failure

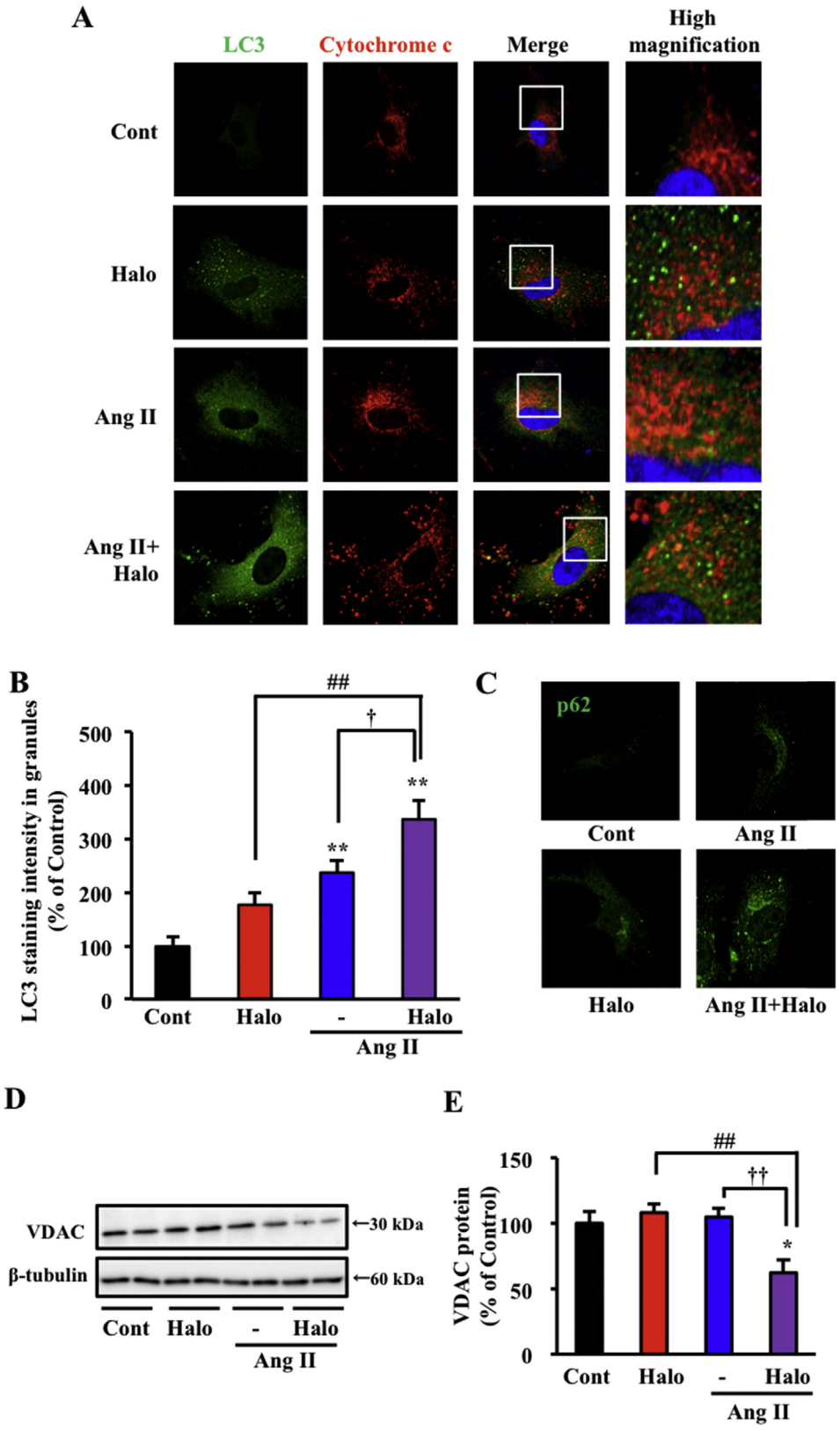

Fig. 4. Effects of haloperidol treatment on autophagy and mitochondrial structure. A: Cultured cardiomyocytes were assessed using antibodies to LC3 (a marker of autophagy; green) and Cytochrome c (a mitochondrial marker; Red) and to DAPI (blue) as a nuclear stain. B: Intensity of LC3 staining in granules is expressed as a percentage relative to control cells. Six to nine randomly selected fields were counted in each experiment. $F(3, 23) = 13.575$, $P < 0.01$. C: Cultured cardiomyocytes were assessed using antibodies to p62 (a marker of autophagy; green). D: Immunoblot of the mitochondrial protein VDAC in cultured cardiomyocytes treated with or without Ang II or Halo for 48 h. E: Quantification by densitometry of VDAC protein. $F(3, 20) = 6.536$, $P < 0.01$. Data are expressed as percentages of control values (mean ± S.E.M.). *, $P < 0.05$ and **, $P < 0.01$ vs. control cells; ##, $P < 0.01$ vs. Halo-treated cells; †, $P < 0.05$ and ††, $P < 0.01$ vs. Ang II-treated cells.

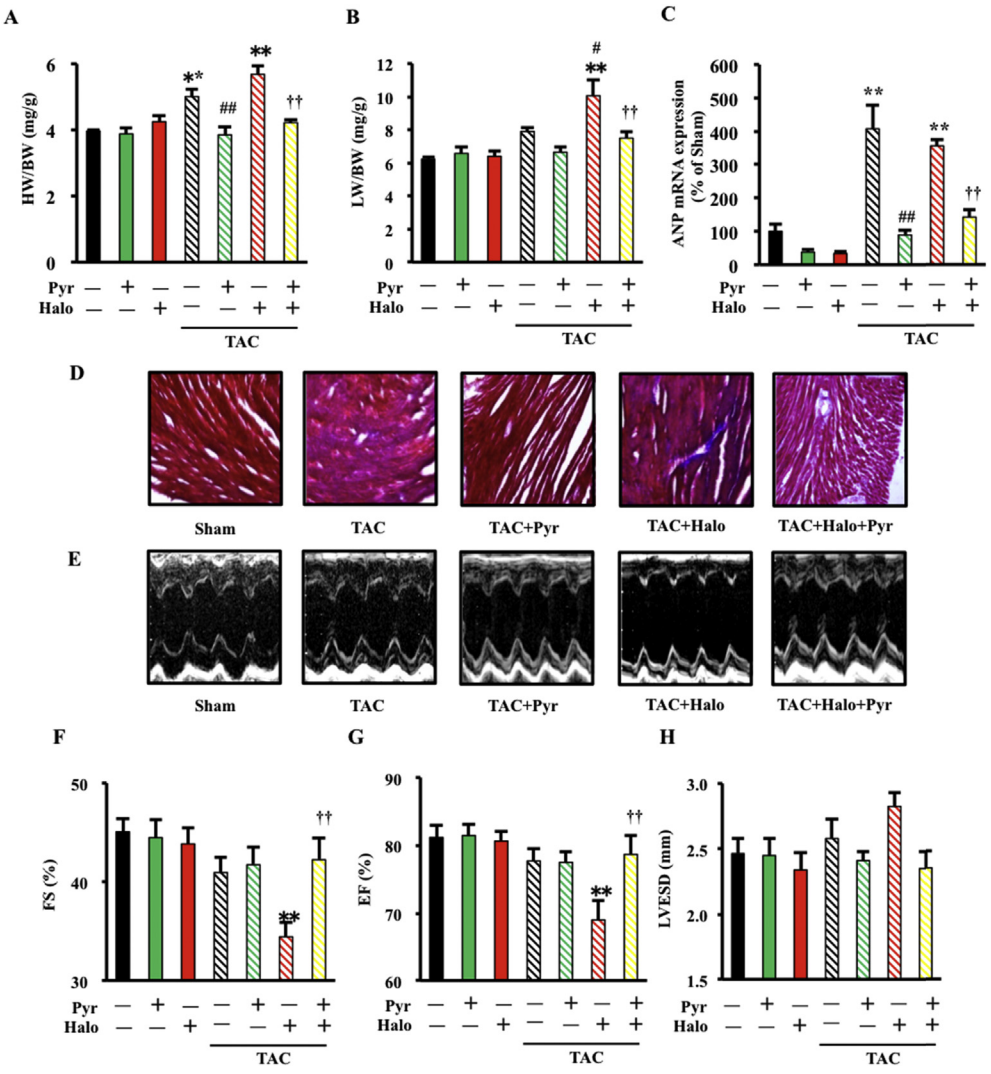

Fig. 5. Effects of haloperidol and sodium pyruvate administration on cardiac hypertrophy and function in TAC mice. A: TAC-induced cardiac hypertrophy, as indicated by the heart weight/body weight (HW/BW) ratio. $F(6, 17) = 14.409$, $P < 0.01$. B: TAC-induced cardiac hypertrophy, as indicated by the lung weight/body weight (LW/BW) ratio. Halo (0.1 mg/kg) and/or sodium pyruvate (1 mg/kg; Pyr) were administered to sham and TAC mice for 2 weeks after surgery. $F(6, 18) = 7.425$, $P < 0.01$. C: Effect of Halo and Pyr treatment on ANP mRNA levels in TAC and control mice. $F(6, 55) = 24.810$, $P < 0.01$. D: Effect of Halo and Pyr on scar formation induced by TAC (Masson's trichrome staining). E: Representative M-mode echocardiograms of TAC mice treated with and without Halo and Pyr. F: Changes in percentage of LV fractional shortening (FS). $F(6, 43) = 3.804$, $P < 0.01$. G: Changes in percentage of ejection fraction (EF). $F(6, 44) = 3.934$, $P < 0.01$. H: Changes in left ventricular end-systolic diameter (LVESD). $F(6, 44) = 1.961$, $P = 0.0920$. Groups consist of 5–9 mice. Each column represents the mean ± S.E.M. **, $P < 0.01$ vs. sham/vehicle-treated group; #, $P < 0.05$ and ##, $P < 0.01$ vs. TAC/vehicle-treated group; ††, $P < 0.01$ vs. TAC/Halo-treated group.

and adverse myocardial remodeling. Several lines of evidence suggest that haloperidol and its more active metabolite irreversibly inhibit σ_1R activity and reduce σ_1R expression levels *in vivo* (17,32,52). Although haloperidol treatment was previously reported to have deleterious effects in heart (34), the molecular mechanisms underlying these effects remained obscure. Here we report that i) chronic haloperidol treatment decreases σ_1R expression, ii) decreases myocardial ATP content, and iii) promotes adverse myocardial remodeling and deterioration of cardiac function, which ultimately led to increased mortality of TAC mice. Combining σ_1R agonists with ATP supplementation, we confirmed that the deleterious effects of chronic haloperidol treatment are mediated by both σ_1R inactivation and impaired mitochondrial ATP production.

Here we address mechanisms underlying deleterious effects of haloperidol on cardiac hypertrophy *in vitro* and *in vivo*. We report that haloperidol treatment impairs ATP production in part by deregulating IP_3R-mediated Ca^{2+} mobilization into mitochondria. Earlier studies in CHO cells demonstrated that σ_1R interacts with IP_3R to form a functional complex to regulate Ca^{2+} entry into mitochondria, enabling cell survival under stress conditions (22). In fact, we previously reported that σ_1R interacts with IP_3R in cardiomyocytes and that σ_1R activation promotes ATP synthesis by enhancing Ca^{2+} entry into mitochondria (44,50). Here, we confirm that σ_1R function is cardioprotective in studies showing that σ_1R inhibition by haloperidol decreases mitochondrial ATP content: haloperidol treatment significantly suppressed PE- and ATP-induced mitochondrial Ca^{2+} transport and potentiated PE- and ATP-induced Ca^{2+} release to the cytosol. Treatment with the selective σ_1R agonist SA4503 completely reversed haloperidol-induced impairment in Ca^{2+} mobilization.

We also show that treatment of cardiomyocytes with both haloperidol and Ang II induces apoptosis, as indicated by the presence of TUNEL-positive cells, and deregulates autophagy, as

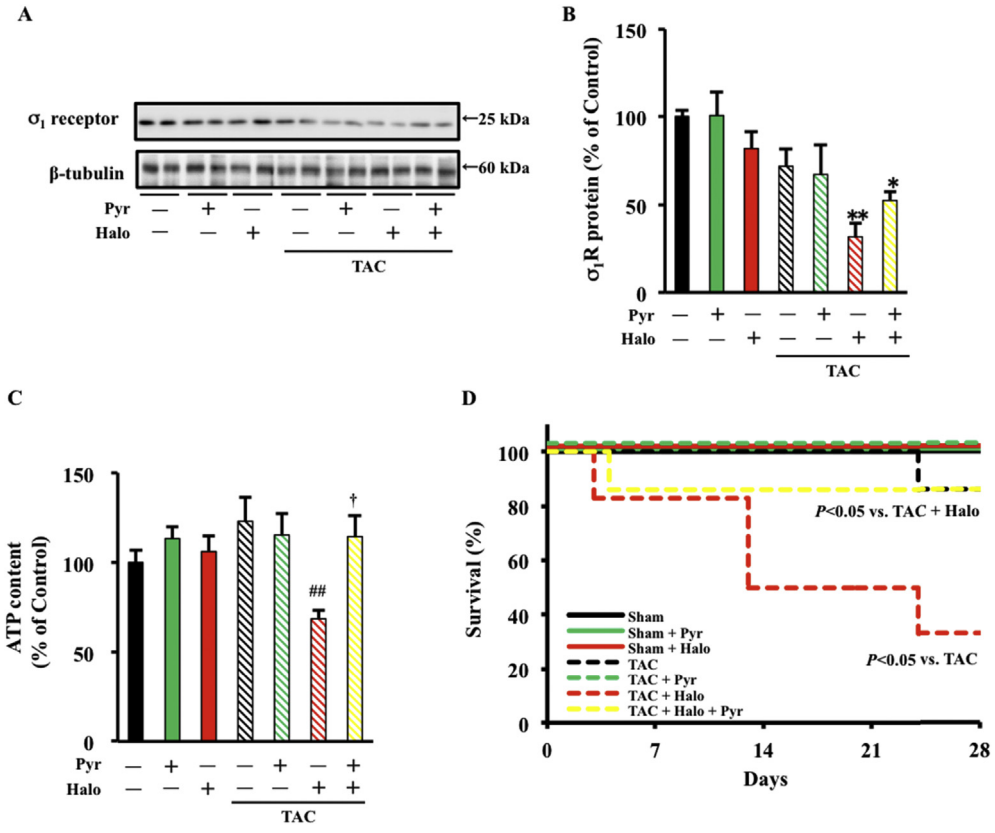

Fig. 6. Effects of combining haloperidol with sodium pyruvate treatment on cardiac σ_1R expression, ATP content and survival in TAC mice. A: Western blot analysis of σ_1R protein in the LV of sham and TAC mice, with or without drug treatment. Anti-β-tubulin staining serves as a loading control. B: Quantification by densitometry of σ_1R immunoreactive bands. $F(6, 19) = 6.005$, $P < 0.01$. C: ATP content in left ventricles with or without drug treatment. $F(6, 34) = 3.436$, $P < 0.01$. *, $P < 0.05$ and **, $P < 0.01$ vs. sham/vehicle-treated group; ##, $P < 0.01$ vs. TAC/vehicle-treated group; †, $P < 0.05$ vs. TAC/Halo-treated group. D: Kaplan–Meier survival analysis following Halo and Pyr treatment of TAC mice. Halo and/or Pyr or saline along were administered once daily to sham and TAC mice and survival was monitored over 28 days. In the Log-rank test: $P < 0.05$ for TAC/Halo vs. TAC/vehicle-treated group; $P < 0.05$ for TAC/Halo/Pyr-treated group vs. TAC/Halo-treated group.

evidenced by increased accumulation of LC3 puncta and p62 upregulation. Currently it is unclear whether autophagosome accumulation occurs as a compensatory mechanism to allow cellular survival under reduced ATP conditions. Interestingly, we also observed increased mitochondrial fragmentation or degradation, as indicated by decreased Mito Tracker intensity, increased LC3/cytochrome c co-localization and decreased VDAC expression, suggesting that mitochondrial dysfunction occurs as cardiac hypertrophy progresses to heart failure. These observations suggest that mitochondrial damage triggers apoptosis or autophagy associated with mitochondrial energy depletion (21). We also found that haloperidol treatment remarkably reduced mitochondrial membrane potential and enhanced similar effects triggered by Ang II treatment. Ang II exposure generates reactive oxygen species (ROS) via activation of NADPH oxidase in vascular smooth muscle and mouse heart (9,37), perturbing mitochondrial function (11,20). Similarly, haloperidol treatment reportedly increases the presence of ROS in neurons (39). These reports suggest that Ang II treatment generates mitochondrial ROS via independent mechanisms. Further studies are required to define mechanisms underlying these outcomes in heart.

We also observed significantly increased mortality in haloperidol-treated TAC mice, with a survival rate of 50% at 14 days and 33% at 28 days as opposed 86% survival at 28 days seen in TAC only mice. Mitochondria comprise approximately 30% of the volume of cardiac muscle. About 70% of ATP generated in heart serves to fuel contraction, and the remaining 30% provides energy for various ion pumps including the Ca^{2+}-ATPase in SR (SERCA) (19,43). Cardiac contraction requires ATP production, and impairment in this process rapidly induces contractile dysfunction (15). Consistent with these findings, we found that haloperidol treatment in TAC mice decreased ATP production and contractile dysfunction. However, haloperidol treatment of sham mice had no *adverse* effect on cardiac morphology and function. This result agrees with a previous report that a total cumulative dose of intravenous haloperidol of <2 mg is safe for use for patients who lack cardiovascular risk factors (34).

Earlier studies of schizophrenia patients combining haloperidol treatment with supplementation with ω-3 polyunsaturated fatty acid, vitamin E and vitamin C support the idea that potential deleterious effects of haloperidol could be ameliorated by reducing oxidative stress (41). Here, we suggest a novel mechanism of ATP supplementation using sodium pyruvate, the end product of glycolysis and substrate for acetyl-CoA, combined with haloperidol treatment. Sodium pyruvate is known to be a safe drug (51) and exhibits a cardioprotective effect against ischemia-reperfusion injury in Langendorff-perfused rat hearts (27). Sodium pyruvate also possesses a therapeutic potential to treat mitochondrial disease (28). Interestingly, sodium pyruvate combined with haloperidol in TAC mice blocked adverse myocardial remodeling, perturbed heart function and progression of heart failure and ultimately increased animal survival by rescuing mitochondrial ATP levels. Moreover, administration of intracoronary pyruvate at supraphysiological concentrations increases cardiac output and

decreases pulmonary capillary-wedge pressure and heart rate in patients with dilated cardiomyopathy and heart failure (25). Indeed, sodium pyruvate treatment reportedly induces mitochondrial biogenesis (54) and can replenish pools of Krebs cycle intermediates, enhancing oxidative phosphorylation (13). These reports support our result that sodium pyruvate prevents haloperidol-induced progression of heart failure by protecting mitochondrial function.

5. Conclusions

We have demonstrated that haloperidol treatment *in vitro* and *in vivo* significantly decreases expression and activation of cardiac σ_1R under stress conditions, which in turn impaired mitochondrial Ca^{2+} mobilization and decreased ATP content. These activities contribute to adverse cardiac remodeling and deterioration of heart function associated with increased mortality in haloperidol-treated TAC mice. We also reported for the first time that ATP supplementation via sodium pyruvate rescues ATP levels in haloperidol-treated TAC mice, enabling proper cardiac contraction and relaxation. Our study suggests that ATP supplementation could be combined with haloperidol as treatment for serious cases of schizophrenia, a regime that could mitigate haloperidol's adverse effects.

Conflict of interest statement

The authors declare that they have no competing interests.

Acknowledgments

This work was supported in part by grants-in-aid for Scientific Research from the Ministry of Education, Science, Sports and Culture of Japan (Kakenhi 24659024 and 24102505 to K.F.) and the Smoking Research Foundation (to K.F.)

References

(1) Bezprozvanny I. The inositol 1,4,5-trisphosphate receptors. Cell Calcium. 2005;38:261–272.
(2) Bhuiyan MS, Fukunaga K. Stimulation of sigma-1 receptor signaling by dehydroepiandrosterone ameliorates pressure overload-induced hypertrophy and dysfunctions in ovariectomized rats. Exp Opin Ther Targets. 2009;13:1253–1265.
(3) Bhuiyan MS, Fukunaga K. Targeting sigma-1 receptor signaling by endogenous ligands for cardioprotection. Exp Opin Ther Targets. 2011;15:145–155.
(4) Bhuiyan MS, Tagashira H, Fukunaga K. Crucial interactions between selective serotonin uptake inhibitors and sigma-1 receptor in heart failure. J Pharmacol Sci. 2013;121:177–184.
(5) Bhuiyan MS, Tagashira H, Fukunaga K. Dehydroepiandrosterone-mediated stimulation of sigma-1 receptor activates Akt-eNOS signaling in the thoracic aorta of ovariectomized rats with abdominal aortic banding. Cardiovasc Ther. 2011;29:219–230.
(6) Bhuiyan MS, Tagashira H, Fukunaga K. Sigma-1 receptor stimulation with fluvoxamine activates Akt-eNOS signaling in the thoracic aorta of ovariectomized rats with abdominal aortic banding. Eur J Pharmacol. 2011;650:621–628.
(7) Bhuiyan MS, Tagashira H, Shioda N, Fukunaga K. Targeting sigma-1 receptor with fluvoxamine ameliorates pressure-overload-induced hypertrophy and dysfunctions. Expert Opin Ther Targets. 2010;14:1009–1022.
(8) Bowen WD, Moses EL, Tolentino PJ, Walker JM. Metabolites of haloperidol display preferential activity at sigma receptors compared to dopamine D-2 receptors. Eur J Pharmacol. 1990;177:111–118.
(9) Byrne JA, Grieve DJ, Bendall JK, Li JM, Gove C, Lambeth JD, et al. Contrasting roles of NADPH oxidase isoforms in pressure-overload versus angiotensin II-induced cardiac hypertrophy. Circ Res. 2003;93:802–805.
(10) Cobos EJ, del Pozo E, Baeyens JM. Irreversible blockade of sigma-1 receptors by haloperidol and its metabolites in guinea pig brain and SH-SY5Y human neuroblastoma cells. J Neurochem. 2007;102:812–825.
(11) de Cavanagh EM, Ferder M, Inserra F, Ferder L. Angiotensin II, mitochondria, cytoskeletal, and extracellular matrix connections: an integrating viewpoint. Am J Physiol Heart Circ Physiol. 2009;296:H550–H558.
(12) Denton RM, Richards DA, Chin JG. Calcium ions and the regulation of NAD+-linked isocitrate dehydrogenase from the mitochondria of rat heart and other tissues. Biochem J. 1978;176:899–906.
(13) Des Rosiers C, Labarthe F, Lloyd SG, Chatham JC. Cardiac anaplerosis in health and disease: food for thought. Cardiovasc Res. 2011;90:210–219.
(14) Di Salvo TG, O'Gara PT. Torsade de pointes caused by high-dose intravenous haloperidol in cardiac patients. Clin Cardiol. 1995;18:285–290.
(15) Doenst T, Nguyen TD, Abel ED. Cardiac metabolism in heart failure: implications beyond ATP production. Circ Res. 2013;113:709–724.
(16) Ela C, Barg J, Vogel Z, Hasin Y, Eilam Y. Sigma receptor ligands modulate contractility, Ca++ influx and beating rate in cultured cardiac myocytes. J Pharmacol Exp Ther. 1994;269:1300–1309.
(17) Eyles DW, Pond SM. Stereospecific reduction of haloperidol in human tissues. Biochem Pharmacol. 1992;44:867–871.
(18) Fayer SA. Torsades de pointes ventricular tachyarrhythmia associated with haloperidol. J Clin Psychopharmacol. 1986;6:375–376.
(19) Gibbs CL. Cardiac energetics. Physiol Rev. 1978;58:174–254.
(20) Goldenberg I, Grossman E, Jacobson KA, Shneyvays V, Shainberg A. Angiotensin II-induced apoptosis in rat cardiomyocyte culture: a possible role of AT1 and AT2 receptors. J Hypertens. 2001;19:1681–1689.
(21) Gomes LC, Di Benedetto G, Scorrano L. During autophagy mitochondria elongate, are spared from degradation and sustain cell viability. Nat Cell Biol. 2011;13:589–598.
(22) Hayashi T, Su TP. Sigma-1 receptor chaperones at the ER-mitochondrion interface regulate Ca(2+) signaling and cell survival. Cell. 2007;131:596–610.
(23) Henderson RA, Lane S, Henry JA. Life-threatening ventricular arrhythmia (torsades de pointes) after haloperidol overdose. Hum Exp Toxicol. 1991;10:59–62.
(24) Hennessy S, Bilker WB, Knauss JS, Margolis DJ, Kimmel SE, Reynolds RF, et al. Cardiac arrest and ventricular arrhythmia in patients taking antipsychotic drugs: cohort study using administrative data. BMJ. 2002;325:1070.
(25) Hermann HP, Pieske B, Schwarzmuller E, Keul J, Just H, Hasenfuss G. Haemodynamic effects of intracoronary pyruvate in patients with congestive heart failure: an open study. Lancet. 1999;353:1321–1323.
(26) Hunt N, Stern TA. The association between intravenous haloperidol and Torsades de Pointes. Three cases and a literature review. Psychosomatics. 1995;36:541–549.
(27) Kerr PM, Suleiman MS, Halestrap AP. Reversal of permeability transition during recovery of hearts from ischemia and its enhancement by pyruvate. Am J Physiol. 1999;276:H496–H502.
(28) Koga Y, Povalko N, Katayama K, Kakimoto N, Matsuishi T, Naito E, et al. Beneficial effect of pyruvate therapy on Leigh syndrome due to a novel mutation in PDH E1alpha gene. Brain Dev. 2012;34:87–91.
(29) Kriwisky M, Perry GY, Tarchitsky D, Gutman Y, Kishon Y. Haloperidol-induced torsades de pointes. Chest. 1990;98:482–484.
(30) Marder SR. Facilitating compliance with antipsychotic medication. J Clin Psychiatry. 1998;59(Suppl. 3):21–25.
(31) Martinet W, Knaapen MW, Kockx MM, De Meyer GR. Autophagy in cardiovascular disease. Trends Mol Med. 2007;13:482–491.
(32) Matsumoto RR, Pouw B. Correlation between neuroleptic binding to sigma(1) and sigma(2) receptors and acute dystonic reactions. Eur J Pharmacol. 2000;401:155–160.
(33) Matsuno K, Nakazawa M, Okamoto K, Kawashima Y, Mita S. Binding properties of SA4503, a novel and selective sigma 1 receptor agonist. Eur J Pharmacol. 1996;306:271–279.
(34) Meyer-Massetti C, Cheng CM, Sharpe BA, Meier CR, Guglielmo BJ. The FDA extended warning for intravenous haloperidol and torsades de pointes: how should institutions respond? J Hosp Med 2010:E8–E16.
(35) Nagai T, Sawano A, Park ES, Miyawaki A. Circularly permuted green fluorescent proteins engineered to sense Ca2+. Proc Natl Acad Sci USA. 2001;98:3197–3202.
(36) Nakai A, Yamaguchi O, Takeda T, Higuchi Y, Hikoso S, Taniike M, et al. The role of autophagy in cardiomyocytes in the basal state and in response to hemodynamic stress. Nat Med. 2007;13:619–624.
(37) Rajagopalan S, Kurz S, Munzel T, Tarpey M, Freeman BA, Griendling KK, et al. Angiotensin II-mediated hypertension in the rat increases vascular superoxide production via membrane NADH/NADPH oxidase activation. Contribution to alterations of vasomotor tone. J Clin Invest. 1996;97:1916–1923.
(38) Reynolds GP, Brown JE, Middlemiss DN. [3H]ditolylguanidine binding to human brain sigma sites is diminished after haloperidol treatment. Eur J Pharmacol. 1991;194:235–236.
(39) Sagara Y. Induction of reactive oxygen species in neurons by haloperidol. J Neurochem. 1998;71:1002–1012.
(40) Shioda N, Ishikawa K, Tagashira H, Ishizuka T, Yawo H, Fukunaga K. Expression of a truncated form of the endoplasmic reticulum chaperone protein, sigma1 receptor, promotes mitochondrial energy depletion and apoptosis. J Biol Chem. 2012;287:23318–23331.
(41) Sivrioglu EY, Kirli S, Sipahioglu D, Gursoy B, Sarandol E. The impact of omega-3 fatty acids, vitamins E and C supplementation on treatment outcome and side effects in schizophrenia patients treated with haloperidol: an open-label pilot study. Prog Neuropsychopharmacol Bol Psychiatry. 2007;31:1493–1499.
(42) Stollberger C, Huber JO, Finsterer J. Antipsychotic drugs and QT prolongation. Int Clin Psychopharmacol. 2005;20:243–251.
(43) Suga H. Ventricular energetics. Physiol Rev. 1990;70:247–277.

(44) Tagashira H, Bhuiyan MS, Fukunaga K. Diverse regulation of IP3 and ryanodine receptors by pentazocine through sigma1-receptor in cardiomyocytes. Am J Physiol Heart Circ Physiol. 2013;305:H1201–H1212.
(45) Tagashira H, Bhuiyan MS, Shioda N, Fukunaga K. Fluvoxamine rescues mitochondrial Ca2+ transport and ATP production through sigma(1)-receptor in hypertrophic cardiomyocytes. Life Sci. 2014;95:89–100.
(46) Tagashira H, Bhuiyan S, Shioda N, Fukunaga K. Distinct cardioprotective effects of 17beta-estradiol and dehydroepiandrosterone on pressure overload-induced hypertrophy in ovariectomized female rats. Menopause. 2011;18:1317–1326.
(47) Tagashira H, Bhuiyan S, Shioda N, Hasegawa H, Kanai H, Fukunaga K. Sigma1-receptor stimulation with fluvoxamine ameliorates transverse aortic constriction-induced myocardial hypertrophy and dysfunction in mice. Am J Physiol Heart Circ Physiol. 2010;299:H1535–H1545.
(48) Tagashira H, Kobori T. [Development of experimental techniques and evaluation to support evidence-based medicine (EBM)]. Yakugaku Zasshi. 2013;133:485.
(49) Tagashira H, Matsumoto T, Taguchi K, Zhang C, Han F, Ishida K, et al. Vascular endothelial sigma1-receptor stimulation with SA4503 rescues aortic relaxation via Akt/eNOS signaling in ovariectomized rats with aortic banding. Circ J. 2013;77:2831–2840.
(50) Tagashira H, Zhang C, Lu YM, Hasegawa H, Kanai H, Han F, et al. Stimulation of sigma1-receptor restores abnormal mitochondrial Ca(2)(+) mobilization and ATP production following cardiac hypertrophy. Biochim Biophys Acta. 2013;1830:3082–3094.
(51) Tanaka M, Nishigaki Y, Fuku N, Ibi T, Sahashi K, Koga Y. Therapeutic potential of pyruvate therapy for mitochondrial diseases. Mitochondrion. 2007;7:399–401.
(52) Usuki E, Bloomquist JR, Freeborn E, Casagnoli K, Van Der Schyf CJ, Castagnoli N. Metabolic studies on haloperidol and its tetrahydropyridinyl dehydration product (HPTP) in C57BL/6 mouse brain preparations. Neurotox Res. 2002;4:51–58.
(53) Vermassen E, Parys JB, Mauger JP. Subcellular distribution of the inositol 1,4,5-trisphosphate receptors: functional relevance and molecular determinants. Biol Cell. 2004;96:3–17.
(54) Wilson L, Yang Q, Szustakowski JD, Gullicksen PS, Halse R. Pyruvate induces mitochondrial biogenesis by a PGC-1 alpha-independent mechanism. Am J Physiol Cell Physiol. 2007;292:C1599–C1605.
(55) Wojcikiewicz RJ. Type I, II, and III inositol 1,4,5-trisphosphate receptors are unequally susceptible to down-regulation and are expressed in markedly different proportions in different cell types. J Biol Chem. 1995;270:11678–11683.
(56) Xiberas X, Martinot JL, Mallet L, Artiges E, Loc HC, Maziere B, et al. Extrastriatal and striatal D(2) dopamine receptor blockade with haloperidol or new antipsychotic drugs in patients with schizophrenia. Br J Psychiatry. 2001;179:503–508.
(57) Zhu H, Tannous P, Johnstone JL, Kong Y, Shelton JM, Richardson JA, et al. Cardiac autophagy is a maladaptive response to hemodynamic stress. J Clin Invest. 2007;117:1782–1793.